Electron Transmission through Self-Assembled Monolayers

Deborah Evans* and Rodric Wampler

Department of Chemistry, University of New Mexico, Albuquerque, New Mexico 87131

Received: December 29, 1998; In Final Form: April 1, 1999

Electron transmission through a series of self-assembled monolayer films is studied using an iterative Green's function method with absorbing boundary conditions. The nuclear-electron interactions are calculated using suitable pseudopotentials, and the Hamiltonian is evaluated using a discrete variable representation. The presence of electronegative head groups on the metal surface gives rise to much lower transmission through the layers. The presence of these headgroups also produces asymmetric transmission effects where the transmission coefficient depends on the incident direction of the electron, as observed in recent STM measurements. Longer alkane chains (up to 18 carbon atoms) are more ordered due to the self-assembly process and have higher transmission coefficients at lower electron energies. This collective effect is observable experimentally and is not a property of single molecules in which transmission probabilities decay roughly exponentially with chain length.

I. Introduction

The possibility of replacing semiconductor devices with organic counterparts has recently become the focus of a great deal of theoretical and experimental interest.[1] Metal/organic film/metal structures about 50−100 Å in length have already been fabricated and display very interesting conductance properties.[2] Their use as molecular scale devices is promising, as it is possible to manipulate the electronic transport properties through the organic films by varying the temperature, molecular disorder, and the presence of solvents.

Electron transfer in condensed phases has been a topic of fundamental experimental and theoretical importance for many years.[3,4] Until recently, these studies have focused on molecular systems where electron transfer from a donor site to an acceptor site occurs with significant coupling of the electron motion to the highly polar solvent medium. Electron transfer rates may be calculated by assuming a nonadiabatic coupling between the Born−Oppenheimer electronic states associated with the donor and acceptor configurations. In general, this nonadiabatic coupling constant is considered to be independent of the solvent motions and nuclear configurations, and in the limit of small couplings, standard second-order perturbation theory may be used to calculate electron transfer rates.

Recently, however, a number of experimental studies have been carried out on systems that do not conform to the above description.[5−9] Electron transmission through thin molecular films adsorbed onto a surface has been examined using a variety of techniques. For example, photoelectron spectroscopy using tunable UV light sources is able to resolve both the energy and momentum[10,11] of electrons photoejected from a metal surface through an absorbed molecular layer. Low-energy electron transmission studies[12] on a variety of adsorbed layers can further probe the effects of layer thickness on electron transmission and relate these to the band structure of the adsorbed layers.[13] Finally, scanning tunneling microscopy can also be used to measure the effects of chain length on electron tunneling probabilities.[14]

Electron transfer through an inherently disordered system, like a liquid or organic thin film, cannot be described in terms of simple adiabatic states that are coupled. Indeed, in these cases, the coupling matrix element, or the transmission probability through a layer is highly dependent on the nuclear configurations of the molecular film. Recent work on electron transmission through thin water layers has shown that this is the case: transmission probabilities are highly dependent on the water configurations, and in some cases water vacancies give rise to long-lived resonances with high transmission probabilities.[15] There is therefore a need to develop theoretical tools to understand these processes for experimentally well-studied systems. To this end, this paper focuses on modeling electron transmission through self-assembled monolayers of thiols adsorbed onto gold surfaces.

Recent experimental studies on electron transport through self-assembled monolayers have yielded a variety of interesting results. The role of molecular order in long-chain organic acids has been measured in photoemission[10] and tunneling[16] experiments. In the presence of higher disorder, the electron transmission decreases.[10] In ordered films, high transmission probabilities are observed even for several monolayers. Electron transfer efficiencies are higher for an all-trans ordered alkane film than a disordered monolayer.[16] These features have been correlated with the band structure in alkane films.[13] In addition, scanning tunneling microscopy on unsaturated thiols have revealed that these films display rectifying properties when adsorbed on a gold surface;[17] electron tunneling probabilities from or toward the metal surface and the STM tip may differ by several orders of magnitude. The rectifying capabilities of the saturated thiols is much smaller.

In this paper, we study electron transmission through thiol monolayers adsorbed onto a gold surface. These thin film structures are generated using classical molecular dynamics simulations, and the electron transmission probabilities through these structures are calculated using an iterative Green's function technique[18] that we discuss in more detail in section II. In section III, we examine the role of molecular configuration and disorder on transmission measurements. Simulations of chains of increasing length were performed in order to relate the film structure to electron transmission properties. The possibility of rectifica-

10.1021/jp984811p CCC: $18.00
Published on Web 05/13/1999

TABLE 1: Molecular Dynamics Parameters[a]

bond stretching[25]			
$^1/_2k(r - r_0)^2$	[k, r_0]		
C−C	[2600, 1.51]	C−S	[1857, 1.81]
bond bending[24]			
$^1/_2\kappa(\theta - \theta_0)^2$	[κ, θ_0]		
C−C−C	[520, 109]	C−C−S	[418, 114.7]
nonbonding[24]			
Lennard-Jones		[ϵ, σ]	
CH_2	[0.598, 3.92]	CH_3	[0.642, 3.74]
S	[1.0468, 3.55]	Au	[0.2328, 3.4]

[a] All energies in kJ/mol, distances in Å, and angles in deg.

tion is also examined for a short chain thiol. In section IV, the dependence of electron transmission probabilities on disorder, chain length, and incident direction are related to the molecular structure. A summary of these effects and further refinements of the model are discussed in the concluding section V.

II. Simulation Models

(i) Molecular Dynamics Simulations. Classical molecular dynamics simulations of monolayers were performed using the parallel DLPOLY algorithm.[19] These simulations were carried out at 200 K in the microcanonical ensemble. The equations of motion were integrated using the leapfrog Verlet algorithm with a 20 fs stepsize and temperature rescaling every 20 steps. The simulations of the thiol films were started from an initially ordered monolayer, positioned with the sulfur on the metal surface and the alkane chains perpendicular to the surface. The alkane chains were in an all-trans configuration. The gold(111) "surface" was made from 600 gold atoms assembled in three layers, and held static throughout the simulation. Initial thiol layers were deposited at surface densities of 1 molecule/22 Å^2, which is a reasonable density based on experimental studies and molecular dynamics simulations of adsorbed thiols centered on the 3-fold hollow sites of the Au[111] surface.

The simulation box was typically 40 Å × 40 Å × 100 Å. The sulfur atoms were allowed to move relative to the gold surface, and periodic boundary conditions were used in the surface direction. Reflecting boundary conditions were used at a distance of 100 Å in the direction of the film growth. These interaction potentials and all others used in the simulation are given in Table 1. Unlike a number of simulations,[20] the sulfur atoms were not constrained to the Au surface. The sulfur−gold interaction potential depth was chosen to correspond to the experimental data obtained from desorption measurements,[21,22] which estimate the covalent bond strength of the Au−S bonds at ≈40 kcal/mol, and to recent ab initio density functional calculations of methanethiol on a Au[111] surface.[23] The potential energy minimum of −12 kcal/mol was set at a distance of 2.25 Å for the sulfur−gold pair potentials used to describe the interaction of the sulfur with an Au atom on the surface. The carbon atoms in the thiols were treated using the united atom approach, and interaction potentials were taken from the work of Tildesley et al.[24] Dihedral potential interactions were taken from the AMBER 4.1 force field.[25] Unlike the above simulations of thiol films, the bond lengths were not constrained and harmonic potentials for these interactions were used with parameters from the AMBER 4.1 force field.[25] Nonbonded interactions between unlike atoms were described using the mixing rules $\sigma_{ij} = (\sigma_i + \sigma_j)/2$ and $\epsilon_{ij} = \sqrt{\epsilon_i \epsilon_j}$.

The equilibration of the surface layers took an average 100−200 ps. After about 50 ps, the longer chains self-assemble and establish a constant tilt angle relative to the surface, as shown for the $C_{12}H_{25}S$−Au film in Figure 1. The short chain thiols

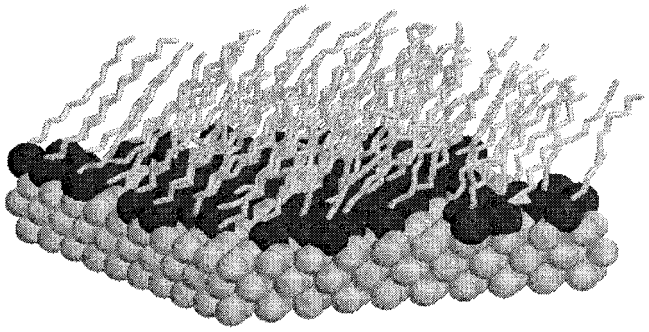

Figure 1. Snapshot of a molecular dynamics simulation of a self-assembled $C_{12}S$−Au monolayer on a Au(111) surface 120 ps along a simulation trajectory.

(C_5- and C_6-thiol) do not, however, self-assemble at these densities. This has important consequences for the electron transmission, as discussed in section III.

(ii) Quantum Transmission Probabilities. The electron transmission problem is inherently quantum mechanical. Calculated transmission data must provide some means of comparison with experimental observables. In a photoelectron experiment, the initial photoejected electron is a nonequilibrium initial state that approaches the thin film barrier (in the simplest case, with a given incident energy and a uniform distribution of initial angular momenta). If the final signal detected is resolved into both energy and momentum components, the monitored signal is directly proportional to $\sum_i |S_{if}|^2$,[26] where S_{if} is the scattering matrix element between the incoming and outgoing electron states $|i\rangle$ and $|f\rangle$. In low-energy electron transmission experiments, the initial state is a single energy and momentum state from a tip that is detected at all possible scattering directions on the metal surface, and the signal is proportional to $\sum_f |S_{if}|^2$.

The energy-resolved photoelectron measurements restrict these states to plane waves of the incoming energy, E, if the electron energies are low enough so as to allow only elastic scattering. Determining the electron flux at the detector can therefore be recast as a scattering problem. Given a final state Ψ_f, the scattering element to the state Ψ_i can be determined using standard scattering formalisms.

New methodologies developed for scattering calculations of molecular systems using absorbing boundary conditions have recently been applied to electron transmission through water layers between two platinum electrodes.[27] The transmission probability is related to $P_f = \sum_i |S_{if}|^2$. This "all-to-one" probability may be calculated from the Green's function on a suitable basis. Given the advancements in solving linear systems, this method has proved to be successful in solving large systems. We have therefore applied this method to the electron transmission through thiol self-assembled monolayers described in the previous section. In order to study several nuclear configurations from an ensemble and perform electron transmission studies for many initial energies, extensive parallelization of the algorithm is also essential.

Using a discrete variable representation (DVR) basis, the incoming wavefunction may be represented on a grid as $|\psi_i\rangle$ and the "one-to-all" probability $P_f(E) = \sum_f |S_{if}|^2$ for electron transmission at an incoming energy E is calculated from[26]

$$P_f(E) = \frac{2}{\hbar} \psi_i^T \cdot \epsilon_i \cdot G^* \cdot \epsilon_f \cdot G \cdot \epsilon_i \cdot \psi_i$$

where $\epsilon_{i,f}(z)$ is the absorbing boundary condition in the transmission direction (z) in either the initial or final scattering space,

respectively. The calculation of transmission probabilities on a suitable basis can therefore be solved by the evaluation of $G|\psi_i\rangle$, where G is the Green's function with absorbing boundary conditions given as $G = 1/(H - E + i\epsilon)$. This linear algebra problem is solved using the generalized minimal residual method [GMRES][28] for non-Hermitian matrices.

Since typical thin film slices measuring 20 Å × 20 Å × 50 Å were taken from the MD simulation data, grid sizes of 16 × 16 × 200 have been used. Grid spacings of 2.5 au were used perpendicular to the transmission direction, and 0.5 au in the direction of transmission, which are many orders of magnitude smaller than the wavelength of the electron at the incoming energies studied. Periodic boundary conditions were enforced perpendicular to the transmission direction. Larger grid sizes in these directions cannot be obtained with the current method, although in the transmission direction, grid sizes of 300 produced the same results. Convergence in the kinetic Hamiltonian in the DVR basis can be obtained by truncation to seventh order. Tunneling probabilities of 10^{-8} are obtained using tolerances in the GMRES routine of 10^{-6}. Absorbing boundary conditions were applied in the transmission direction z and several forms were used, including $\epsilon(z) = \alpha[(z - z_0)/(z_{max} - z_0)]^4$ [with typical values of $\alpha = 0.25$ and $z_{max} = 60$ au], and the Woods−Saxon potential[29] $\epsilon(z) = 2\lambda/\{1 + \exp[(z_{max} - z)/\eta]\}$, when $0 < z$, and a similar function when $0 > z$.

The interaction potential between the electron and molecular thin film was calculated from one-electron pseudopotentials. The carbon atoms in the alkane chains were described using pseudopotentials developed by Berne and Liu.[30] The carbon bond centers were described using a pseudopotential that takes into account repulsion, polarizability, and correlation:

$$V_{e-CH_2}(r) = Ae^{-\alpha r} + Be^{-\beta r} + S(r)$$

with $A = 300$ au, $B = -132$ au, and $\alpha = 2.1$ au, $\beta = 1.87$ au. $S(r)$ is the polarizability function:

$$S(r) = -\lambda\frac{e^2}{2r^4}(1 - e^{-r/r_0})^6$$

with $\lambda = 17.5$ au and $r_0 = 1.175$ au, which is included as an effective two-body interaction.

Following Berne and Liu, the midpoint of each C−C bond is treated as a repulsive pseudopotential center:

$$V_{e-M}(r) = Ae^{-\alpha r}$$

with $A = 165$ au and $\alpha = 2$ au.

The heteroatom pseudopotentials are intended to mimic the behavior of an electronegative headgroup. These were based on the pseudopotentials of the oxygen in methanol[31] and water.[32] These have been modified by increasing the polarizability to correspond to that of sulfur instead of oxygen. The Coulomb part of the pseudopotential is in fact taken to be the same as that in the water molecule; in self-assembled monolayers, the thiols are chemisorbed onto the gold surface and the sulfur atom is negatively charged. While these parameters are introduced to describe surface atoms with higher electronegativity and polarizability than the carbon centers, they do *not* accurately describe the potential of a sulfur atom chemisorbed onto a gold surface. If this data were to be accessed it would require large scale density functional modeling of the gold surface and the adsorbed sulfur species. As far as we are aware, this has not yet been done. Our studies have therefore used a pseudopotential form appropriate for describing a model thin film with large electronegative headgroups attached to a metal surface, namely

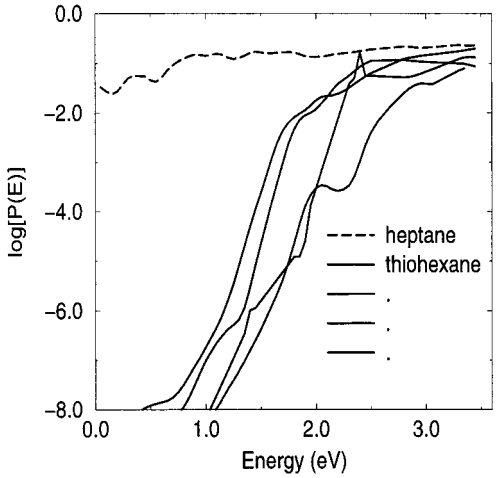

Figure 2. Transmission probability $P(E)$ vs the electron energy for several thiohexane thin film structures (taken at 50 ps snapshots along a simulation trajectory, solid lines) is compared with heptane where the sulfur pseudopotential is replaced by that of carbon.

$$V_{e-S}(r) = \frac{2Z_e}{|r - R_s|} + V_0e^{-\alpha_s|r-R_s|} + S(r)$$

with $Z_e = 0.329e$ and V_0 and α_s the parameters used for the oxygen (at position R_s) in the water pseudopotential.[32]

The polarizability function is included as a two-body interaction potential:

$$S(r) = -\lambda\frac{e^2}{2r^4}(1 - e^{-r/r_0})^6$$

with $\lambda = 21.7$ au scaled to correspond to the increased polarizability of the sulfur atom, and r_0 chosen to be the size of a SH headgroup, as suggested by Trular et al. and Burke et al.,[33] in much the same way the OH group is treated in methanol with numbers adjusted accordingly.

III. Results

The role of the surface heteroatoms on the electron transmission is expected to be important. The polar headgroups are much more effective at scattering the electrons, and thin thiol films allow much lower transmission than the alkanes at these incident electron energies. Figure 2 shows the electron transmission of a photoejected electron of energy E above the vacuum level for heptane and thiohexane. Several different nuclear configurations from an equilibrated thiohexane film are shown. While there are some differences for film structures 50 ps apart on a simulation trajectory, the overall transmission profile is rather similar in terms of the energies at which the transmission probability approaches values of order unity. The heptane transmission data are obtained by using one of these classical thiohexane nuclear configurations and replacing the heteroatom pseudopotential by that of carbon. Although the heptane layer is artificial, it enables us to directly assess the effects of the heteratom on electron transmission without a change in nuclear conformation.

The effect of the headgroups and the inherent disorder of their arrangement on the surface is also shown in Figure 3. Transmission probability through a thiohexane film is shown from both incident directions: through the thiol groups first (as in photoelectron experiments) and through the carbon chains

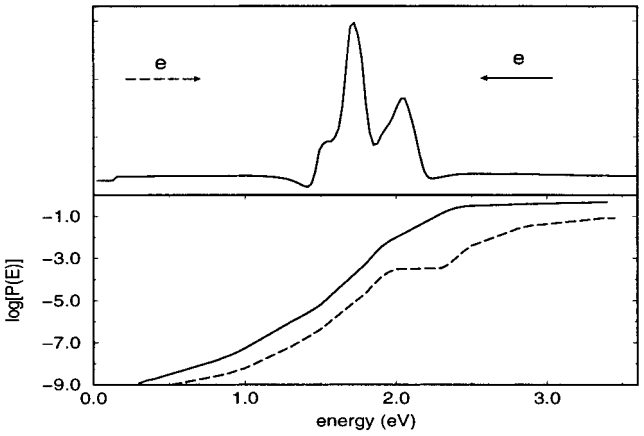

Figure 3. Thiohexane monolayer exhibiting asymmetric tunnel probability $P(E)$ for a range of incident electron energies. The effective electron potential $V(z)$ vs the tunneling direction z in (a) shows the incident electron direction for the probabilities $P(E)$ shown in (b). The probabilities incident through the sulfur monolayer (dashed line) are a couple of orders of magnitude lower than incident through the organic residues.

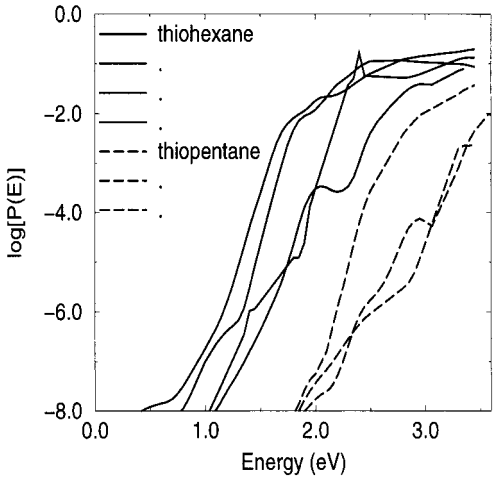

Figure 4. Comparison of transmission probabilities $P(E)$ vs electron energy for several thiopentane structures along a classical molecular dynamics simulation trajectory (dotted lines) and several thiohexane configurations (solid lines). The effective barrier to transmission is much higher for thiopentane.

first (as in LEET experiments). The electron transmissions differ by about 1 or 2 orders of magnitude over this energy range. This "thin-film lens" property is entirely analogous to the effect in thin water films[27] and arises from the nature of the measurement [the "one-to-all" transmission probability] and the disorder of the sulfur atoms on the metal surface.

A number of recent STM studies focused on chain length effects in single molecule electron transfer.[14] Theoretical models of single molecular wires[34] have been used to understand these results and calculate the rate of exponential decay of electron transmission with chain length. Our studies have focused on a different problem: electron transmission of photoejected electrons through an array of self-assembled chains. This is no longer a deep tunneling process, and there exists a possibility for correlation effects to play a role, since scattering from an array of linear chains is now possible.

We have studied electron transmission at a number of energies, and for a number of ensemble configurations for a series of alkane thiols. In Figure 4, electron transmission through thiohexane and thiopentane are compared for a number of static configurations along a simulation trajectory. These configurations represent equilibrated structures of thiopentane and thiohexane with a surface coverage of 1 molecule/22 Å^2 in both cases. Despite the shorter chain length, the thiopentane provides a higher effective barrier than the thiohexane. This can be seen by fitting the transmission curves to an effective one-dimensional barrier of 25 Å long [approximately the chain length for thiohexane] and 2.2 eV high, whereas the best-fit data for the thiopentane is 20 Å long and 3.5 eV high. This result is surprising given that we have found a decrease in transmission for similar calculations on a single carbon chain with an increasing number of carbon atoms. Examination of our classical molecular dynamics data shows that at the surface coverages we are looking at, these shorter chain thiols do not self-assemble, but there are significant numbers of alkane chains lying flat on the surface. In the case of the shorter thiopentane chains, the sulfur atoms tend to cluster closer on the surface, and since the heteroatoms are the most important scattering cores, the transmission is decreased. The electron potential at a height of 2.0 Å above the metal surface is shown for both these systems in Figure 5. The thiopentane potential slice shown in (a) illustrates that, closer to the surface, the sulfur atoms are clustered together more than for the thiohexane shown in (b).

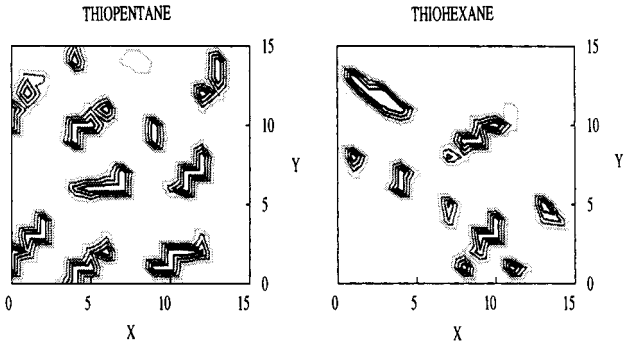

Figure 5. Slice of electronic potential $V(x,y)$ parallel to the gold surface at a height of 2 Å for thiopentane and thiohexane monolayers.

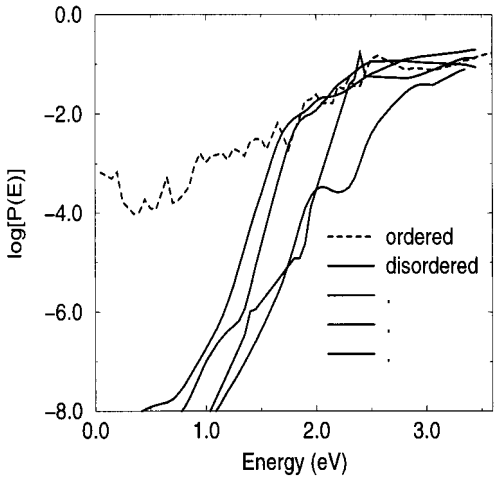

Figure 6. Comparison of transmission probabilities $P(E)$ vs electron energy for ordered thiohexane films with all molecules perpendicular to the metal surface and several disordered monolayer configurations (solid lines) along a simulation trajectory.

The inherent order in the layers is of great interest to the photoelectron transmission experiments. In Figure 6, an ordered layer of thiohexane (at the simulation start with all chains perpendicular to the metal surface) is compared with the equilibrated film, which for this short chain is not a self-assembled monolayer. The disordered layers have lower transmission probabilities than the ordered configuration, in quali-

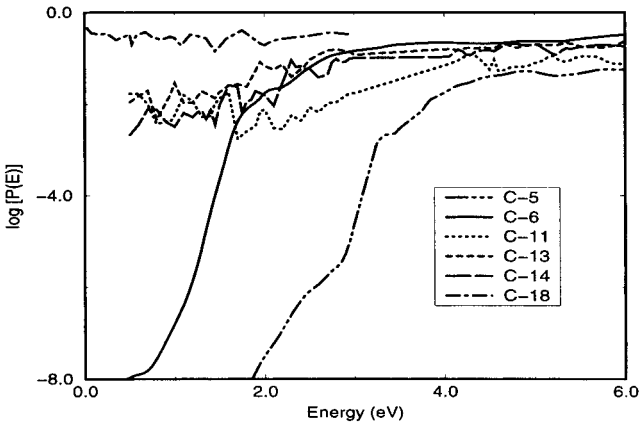

Figure 7. Comparison of transmission probabilities $P(E)$ vs electron energy for longer chain thiols.

tative agreement with the earlier data on stearic acid films on metal surfaces.[10,35]

Order effects manifest themselves most interestingly in the case of the longer chain monolayers. Our simulation data show that for all chains longer than thiohexane, the films self-assemble with a measurable tilt angle that varies between 15 and 30°. In particular, the alkane chains are rather ordered with most bonds in the anti configuration. As shown in Figure 7, the longer chains show surprisingly high electron transmission, especially at lower electron energies. For the highly ordered self-assembled monolayers, the electron transmission may be facilitated by the presence of a well-developed band structure. In fact, this effect has been seen for experimental data on long chain organic acids.[35] Further corroboration is obtained from secondary electron emission measurements on a series on alkane thiols deposited on gold surfaces.[36] The presence of a well-developed band structure is demonstrated by narrow resonance peaks for $C_{18}S-$ films in contrast to the C_6S- films. This many-body cooperative effect is not seen in experiments or calculations through single molecular wires. However, when a sufficient number of chains are assembled, the overlap of their wavefunctions and the formation of accessible bands for an electron may lead to results not obtained for single molecules.

IV. Discussion

Our studies described above have focused on the effects of molecular structure on electron transmission probabilities in thin films. They clearly show that the molecular configuration in thin films is the most important factor in determining the tunneling matrix element. Thus, neither Marcus theory nor continuum theories currently used to understand electron transmission in thin amorphous films are expected to be particularly relevant or accurate for describing electron transmission experiments in self-assembled monolayers. Continuum dielectric modeling of thin films is unable to capture the effects induced by molecular disorder and in self-assembled monolayers describes the influence of strongly polar headgroups absorbed on the metal surface.

We have found that the presence of heteroatoms on the metal substrate surface leads to a sharp dependence of the conducting properties of the thin film on the disorder and arrangement of the sulfur atoms. The polarity of these headgroups is responsible for the sharply decreased electron transmission when thiohexane replaces heptane as the surface absorbate. The spatial arrangement of these headgroups also leads to an increased effective barrier provided by thiopentane layers compared with thiohexane layers. Neither of these shorter thiols self-assemble on the substrate surface. In thiopentane, the shorter alkyl chain enables the sulfur atoms to aggregate in pockets on the surface, where the sulfur density is much higher. This leads to a higher effective potential barrier, and hence lower transmission despite the shorter chain length of thiopentane.

The transmission process is also inherently three-dimensional and therefore these properties are not easily described by continuum thin film slabs. The presence of three-dimensional scatterers causes these thin films to behave as molecular-scale rectifiers: electron transmission through a thiol thin film depends on the incident direction, in sharp contrast to one-dimensional systems where this is expected to be an equivalent scattering process. This same property has also been found in thin water films,[27] but its manifestation in SAMs may, however, prove to be fruitful in the design of alternative molecular scale devices, since thin-film sandwich devices have already been manufactured experimentally. This rectification of current due to the inherent three-dimensional disorder and presence of polar headgroups is an entirely different mechanism from the single molecule rectifiers proposed earlier[37] based on a tunneling process and resonance with the molecular orbitals.

Comparison of highly ordered thiohexane films with the simulated layers shows that an increase in order comes with a concomitant increase in electron transmission. Especially at lower energies, the conducting properties are highly dependent on this structural order. The effects of the order in a self-assembled monolayer are demonstrated most clearly for the longer chain thiols. Enhanced transmission is observed for all chains that our simulations predicted to self-assemble (i.e., longer than thiohexane). The prediction of a higher degree of order in the longer self-assembled chains is in agreement with recent experimental results that show the band structure of $C_{18}S-$ layers to be extremely well-developed. The collective phenomenon and its effects on the electron transmission are, however, very interesting.

Experimental studies on self-assembled carboxylic acids have demonstrated that electron transmission through thin monolayers decreases as the layers become more disordered.[10] Our calculations on thiohexane in an ordered (crystalline) and disordered configuration have shown this to indeed be true. Our results on the longer more ordered self-assembled monolayers have also shown this to be the case. These transmission properties have been observed in electron transmission experiments of C_{18}-mercaptan monolayers.[36] The experiments have, however, revealed more details not captured by our simulations: experimentally, at some energy (10 eV) the transmission again drops as, presumably, a band gap is reached. In our simulation results we have not yet been able to capture this high-energy behavior. A number of possible reasons to explain this exist: (1) Our simulations do not take into account many-body polarizability effects. These may be essential in capturing this collective phenomenon. (2) While our simulation parameters are meant to describe a system with carbon centers and heteroatoms on the surface of a metal, the pseudopotentials of the sulfur atoms on the gold are rather crude. They do not take into account charging effects, or image potentials, and in principle, accurate electronic structure calculations to obtain accurate pseudopotentials at the surface may be required to obtain quantitative agreement in the drop off of transmission probability at higher energies. Our pseudopotentials may indeed push the band gap to higher values than in the real system and are therefore not observed for the energy range of our calculation.

Our study has extended electron transmission studies to self-assembled monolayers and has illustrated interesting behavior

not apparent from single molecule calculations. The role of disorder and molecular configuration have led to interesting dependences of the electron behavior on SAM chain length not expected from single-molecule tight binding calculations. More sophisticated pseudopotentials (even within the one-electron transmission model) are expected to yield new and exciting results and quantitative agreement with experimental numbers. Improving on these preliminary results using DFT calculations is therefore the next step in obtaining quantitative agreement with experimental results. The details of the electron density at the metal−SAM interface and the presence of image potentials are also expected to influence electron transmission. Addressing these topics is of interest to others studying thin film electronic structure[38] and it is an obvious extension of the studies described in this paper and therefore the focus of our current studies on electron transport in thin films.

Acknowledgment. The authors gratefully acknowledge the financial support of the ACS Petroleum Research Fund [32821-G6], the NSF-REU program and Sandia National Laboratory [SURP program]. Computer resources were provided by the Albuquerque High Performance Computing centre and the Maui High Performance Computing center.

References and Notes

(1) (a) Ghadiri, M. R. *Adv. Mater.* **1995**, *7*, 675. (b) Muller, S.; Schwarz, M. *Z. Phys. B* **1995**, *97*, 503. (c) Miura, N.; Yoshikawa, N.; Sugahara, M. *Appl. Phys. Lett.* **1995**, *67*, 3969. (d) Urbakh, M.; Daikhin, L.; Klafter, J. *J. Chem. Phys.* **1995**, *103*, 10707.

(2) Yu, Z. G.; Smith, D. L.; Saxena, A.; Bishop, A. R. *Phys. Rev. B* **1997**, *56*, 6494.

(3) (a) Marcus, R. A. *Annu. Rev. Phys. Chem.* **1964**, *15*, 155. (b) Marcus, R. A. *J. Chem. Phys.* **1965**, *43*, 679. For applications see, for example, the review: (c) Newton, M.; Sutin, N. *Annu. Rev. Phys. Chem.* **1984**, *35*, 437.

(4) (a) Leggett, A. J.; Chakravarty, S.; Dorsey, A. T.; Fisher, M. P. A.; Garg, A.; Zwerger, W. *Rev. Mod. Phys.* **1987**, *59*, 1. (b) Caldeira, A. O.; Leggett, A. J. *Ann. Phys. (NY)* **1983**, *149*, 374. (c) Makri, N.; Makarov, D. E. *J. Chem. Phys.* **1995**, *102*, 4611. (d) Coalson, R. D. *J. Chem. Phys.*, *J. Chem. Phys.* **1987**, *86*, 995.

(5) (a) Boulas, C.; Davidovits, J. V.; Vuillaume, D. *Phys. Rev. Lett.* **1996**, *76*, 4797. (b) Vuillaume, D.; Boulas, C.; Rondelez, F. *Appl. Phys. Lett.* **1996**, *69*, 1646.

(6) Han, E-M.; Do, L-M.; Shirota, Y. *J. Appl. Phys.* **1996**, *80*, 3297.

(7) Bumm, L.; Arnold, J.; Cygan, M.; Dunbar, T.; Burgin, T.; Jones, L.; Allara, D.; Tour, J.; Weiss, P. *Science* **1996**, *271*, 1705.

(8) Shachal, D.; Manassen, Y. *Chem. Phys. Lett.* **1997**, *271*, 107.

(9) Tans, S. J.; Devoret, M. D.; Dal, H.; Thess, A.; Smalley, R.; Geerligs, L. J.; Dekker, C. *Nature* **1997**, *386*, 475.

(10) (a) Kadyshevitch, A.; Naaman, R. *Thin Solid Films* **1996**, *288*, 139. (b) Kadyschvitch, A.; Naaman, R. *Phys. Rev. Lett.* **1995**, *74*, 3443.

(11) Kadyshevitch, A.; Ananthavel, S. P.; Naaman, R. *J. Chem. Phys.* **1997**, *107*, 1288.

(12) (a) Michaud, M.; Cloutier, P.; Sanche, L. *Phys. Rev. B* **1991**, *44*, 10485. (b) Nagesha, K.; Gamache, J.; Bass, A. D.; Sanche, L. *Rev. Sci. Instrum.* **1997**, *68*, 3883. (c) Steinberger, I. T.; Bass, A. D.; Shechter, R.; Sanche, L. *Phys. Rev. B* **1993**, *48*, 8290.

(13) Sanche, L. *Phys. Rev. Lett.* **1995**, *75*, 2904.

(14) (a) Cygan, M. T.; Dunbar, T. D.; Arnold, J. J.; Bumm, L. A.; Shedlock, N. F.; Burgin, T. P.; Jones, L., II; Allara, D. L.; Tour, J. M.; Weiss, P. S. *J. Am. Chem. Soc.* **1998**, *120*, 2721. (b) Weiss, P. S.; Bumm, L. A.; Dunbar, T. D.; Burgin, T. P.; Tour, J. M.; Allara, D. L. *Ann. N. Y. Acad. Sci.* **1998**, *852*, 145.

(15) Galperin, M.; Nitzan, A.; Peskin, U. Manuscript in preparation.

(16) Haran, A.; Waldeck, D. W.; Naaman, R.; Moons, E.; Cahen, D. *Science* **1994**, *263*, 948.

(17) Dhirani, A.; Lin, P.; Guyot-sionnest, P.; Zehner, R.; Sita, L. *J. Chem. Phys.* **1997**, *106*, 5249.

(18) Haran, A.; Kadyshevitch, A.; Cohen, H.; Naaman, R.; Seiderman, T.; Evans, D.; Nitzan, A. *Chem. Phys. Lett.* **1997**, *268*, 475.

(19) DLPOLY is a package of molecular simulation routines written by W. Smith and T. R. Forester (copyright The Council for the Central Laboratory of the Research Councils, Daresbury Laboratory at Daresbury, Nr. Warrington (1996)).

(20) See, for example: Mar, W.; Klein, M. *Langmuir* **1994**, *10*, 188.

(21) Nuzzo, R. G.; Zegarski, B.; Dubois, L. H. *J. Am. Chem. Soc.* **1987**, *109*, 733.

(22) (a) Hautman, J.; Klein, M. L. *J. Chem. Phys.* **1989**, *91*, 4995. (b) Mar, W.; Klein, M. L. *Langmuir* **1994**, *10*, 188.

(23) (a) Beardmore, K.; Kress, J. D.; Gronbechjensen, N.; Bishop, A. R. *Chem. Phys. Lett.* **1998**, *286*, 40. (b) Beardmore, K.; Kress, J. D.; Bishop, A. R.; Gronbechjensen, N. *Synth. Met.* **1997**, *84*, 317.

(24) Moller, M. A.; Tildesley, D. J.; Kim, K. S.; Quirke, N. *J. Chem. Phys.* **1991**, *94*, 8391.

(25) Pearlman, D. A.; Case, D. A.; Caldwell, J. W.; Ross, W. S.; Cheatham, T. E., III; Ferguson, D. F.; Seibel, G. L.; Singh, U. C.; Weienr, P. K.; Kollman, P. A. *AMBER 4.1*, University of California: San Francisco, 1995.

(26) Naaman, R.; Haran, A.; Nitzan, A.; Evans, D.; Galperin, M. *J. Phys. Chem. B* **1998**, *102*, 3658.

(27) (a) Benjamin, I.; Evans, D. G.; Nitzan, A. *J. Chem. Phys.* **1997**, *106*, 6647. (b) Benjamin, I.; Evans, D. G.; Nitzan, A. *J. Chem. Phys.* **1997**, *106*, 1291.

(28) (a) Saad, Y. *Iterative methods for sparse linear systems*; PWS Publishing Co.: Boston, 1996. (b) Tal-Ezer, H. A modified GMRES algorithm. To be published.

(29) (a) Manthe, U.; Seideman, T.; Miller, W. H. *J. Chem. Phys.* **1994**, *101*, 4759. (b) Seideman, T.; Miller, W. H. *J. Chem. Phys.* **1992**, *96*, 4412. (c) Seiderman, T.; Miller, W. H. *J. Chem. Phys.* **1992**, *97*, 2499.

(30) Liu, Z.; Berne, B. J. *J. Chem. Phys.* **1993**, *99*, 9054.

(31) Hilczer, M.; Bartczak, W.; Sopek, M. *J. Phys. Chem.* **1992**, *96*, 2736.

(32) Wallqvist, A.; Thirumalai, D.; Berne, B. *J. Chem. Phys.* **1987**, *86*, 6404.

(33) Burke, P. G.; Chandra, N. *J. Phys. B* **1972**, *5*, 1696. Trular, D. G.; Dixon, D. A.; Eades, R. A. In *Electron-molecule and photon-molecule collisions*; Resigno, T. N., McCoy, V., Schneider, B., Eds.; Plenum: New York, 1979.

(34) (a) Olsen, M.; Mao, Y.; Windus, T.; Kemp, M.; Ratner, M.; Leon, N.; Mujica, V. *J. Phys. Chem.* **1998**, *B102*, 941. (b) Roitberg, A.; Ratner, M. A. *J. Phys. Chem.* **1996**, *100*, 8349. (c) Mujica, V.; Kemp, M.; Ratner, M. *J. Chem. Phys.* **1996**, *104*, 7296.

(35) (a) Kadyshevitch, A.; Naaman, R. *Surf. Interface Anal.* **1997**, *25*, 71. (b) Naaman, R.; Haran, A.; Nitzan, A.; Evans, D.; Galperin, M. *J. Phys. Chem. B* **1998**, *102*, 3658.

(36) (a) Haran, A.; Naaman, R. *Temperature dependence of electron transmission through organized organic thin films*. Presented at Electron Transmission through Molecules and Molecular Interfaces, Maagan, December 1998. (b) Naaman, R.; Kadushevitch, A.; Haran, A.; Ananthavel, S. *Abstr. Pap.—Am. Chem. Soc.* **1997**, No. 214, 49-PHYS.

(37) Aviram, A.; Ratner, M. A. *Chem. Phys. Lett.* **1974**, *29*, 277.

(38) Friesner, R. A.; Beachy, M. D. *Curr. Opinion Struct. Biol.* **1998**, *8*, 257.